J-T CHARACTERIZATION OF ELASTIC-PLASTIC STRESS FIELDS IN A MODE II CRACK SPECIMEN

M.R. Ayatollahi
Fatigue and Fracture Lab., Department of Mechanical Engineering
Iran University of Science and Technology
Narmak, Tehran, 16844, Iran
m.ayat@iust.ac.ir

Abstract

Previous studies on the effects constraint in elastic plastic fracture mechanics are mainly confined only to mode I cracks. Very little research has been carried out to study the effects of constraint on mode II brittle fracture. In this research the variation of Q_{II} with applied load is obtained for a mode II specimen. The specimen is simulated by the finite element method to determine the extent of validity of Q_{II} determined from the *Q-T* diagram. The constraint parameter Q_{II} obtained from the finite element results (or the full field solution) is compared with Q_{II} predicted using the *Q-T* diagram. It is shown that the results of the full field solution are in good agreement with those of the *Q-T* diagram, but only for low levels of load. For higher loads the discrepancy between the results of two methods becomes significant.

Introduction

Elastic-plastic fracture mechanics (EPFM) deals with cracked specimens in which a significant volume around the crack tip undergoes plastic deformation prior to initiation of fracture. For such cases, which very often happen for metallic alloys, the failure mechanism can be either brittle fracture or ductile failure. For specimens failing by the mechanism of brittle fracture, the unstable fracture takes place when the path independent integral J attains a critical value J_c which is a material property. Because the stress field inside the plastic zone near the crack tip is often described by J, the critical value J_c corresponds to the critical stress needed for initiation of crack extension in stress controlled models for brittle fracture.

Mixed mode specimens can also fail by the mechanism of brittle fracture even in the presence of significant plasticity around the crack tip. This has been shown for example through experiments carried out by Maccagno and Knott [1] for several steel alloys. The direction and the onset of crack growth for such cases can often be predicted by using the mixed mode fracture criteria. However, some modifications are needed to account for the effect of crack tip plasticity. For example, the maximum tangential stress (MTS) criterion [2] can be extended to solve the elastic-plastic crack problem in mixed mode loading. Maccagno and Knott [1,3] showed for several steel alloys that the fracture load predicted using the elastic-plastic MTS criterion are in better agreement with the experimental results than those predicted by the linear elastic MTS criterion.

Meanwhile, the experimental studies for mode I cracks show that the fracture toughness obtained from different conventional cracked specimens made of similar material are not the same. This indicates that the fracture toughness or the critical value of J for fracture initiation J_c is not merely a material property but depends also on the geometry and loading configurations. The geometry dependency of fracture toughness can be attributed to the effect of the crack tip constraint. Based on the classical theories of fracture mechanics, the stresses and strains around the tip of a mode I crack can be characterised by a single parameter such as K_I or J. This is true only when certain size restrictions are applied for each crack specimen [4]. However, the geometry dependency of the fracture toughness suggests that at least a second parameter like T or Q is required to predict the critical conditions for crack growth in different specimens [5-7].

Very little research has been carried out to study the effect of constraint in mode II and mixed mode (I/II) loading (see for example [8]). This is partly because of a common assumption that the T-stress is always zero for mode II deformation. Ayatollahi et al. [9,10] have shown that there are many real mode II loading conditions involving significant values of T. The effects of a far field T-stress on the near crack-tip elastic-plastic stresses have been recently investigated for mode II deformation by Ayatollahi et all [11]. Using a mode II constraint parameter Q_{II} , they [11] developed a Q-T diagram to estimate the crack tip constraint from the T-stress. However, it is important to study the range of validity of the J-T formulation using practical crack specimens.

In this paper the constraint parameter Q_{II} is predicted from the Q-T diagram for a mode II specimen. The parameter Q_{II} is also determined directly from the finite element results. These two calculated values of Q_{II} are compared and the related results are discussed.

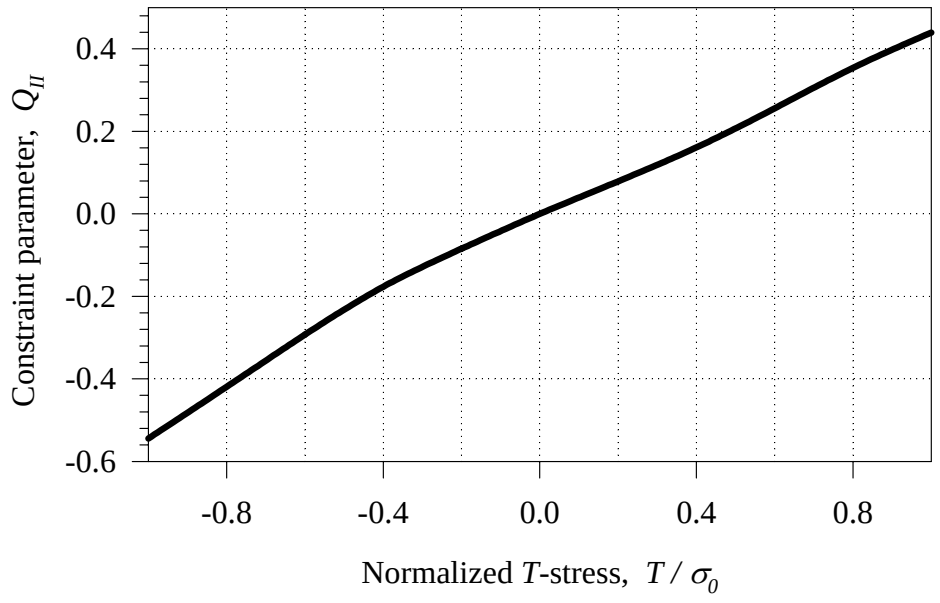

FIGURE 1. Q_{II}-T diagram for n =8 [1].

T-Q relation in mode II

It is common to use a so-called boundary layer model to study the effect of the crack tip parameters on the stresses inside the plastic zone. In the boundary layer model (BLM) a crack is considered in a circular region so that the crack tip is placed in the center of the region. The elastic stresses or displacements corresponding to the singular term and *T* term in the Williams' series expansions are applied to the boundary of the region. Material properties are considered to be elastic-plastic. To ensure the conditions necessary for contained yielding, the magnitudes of the boundary conditions should be limited to a level at which the maximum radius of plastic zone is small compared with the radius of the circular region. If the *T* term on the boundary is zero, the stresses inside the plastic zone are in good agreement with the stresses given by the HRR solution[5-7].

The boundary layer model can also be used for quantifying the crack tip constraint [6,7]. The mode I constraint parameter Q_I corresponding to brittle fracture is determined as

$$Q_I = \frac{\sigma_{\theta\theta} - (\sigma_{\theta\theta})_{REF}}{\sigma_{\circ}} \quad \text{along} \quad \theta = 0 \quad \text{for} \quad 1 \le \frac{r\sigma_o}{J} \le 5 \tag{1}$$

where σ_o is the yield stress, $\sigma_{\theta\theta}$ is the tangential stress and $(\sigma_{\theta\theta})_{REF}$ is either the HRR solution for mode I or the boundary layer solution for small scale yielding with T=0. A similar formulation can be used to determine Q_{II} for mode II cracks [11]. However, in this case, brittle fracture no longer takes place along the crack line. If the maximum tangential stress (MTS) criterion [2] is adopted for predicting the direction of fracture initiation, the crack tip constraint should be studied along the direction of maximum tangential stress θ_o around the crack tip. Therefore, the constraint parameter in brittle fracture for mode II loading Q_{II} can be determined from

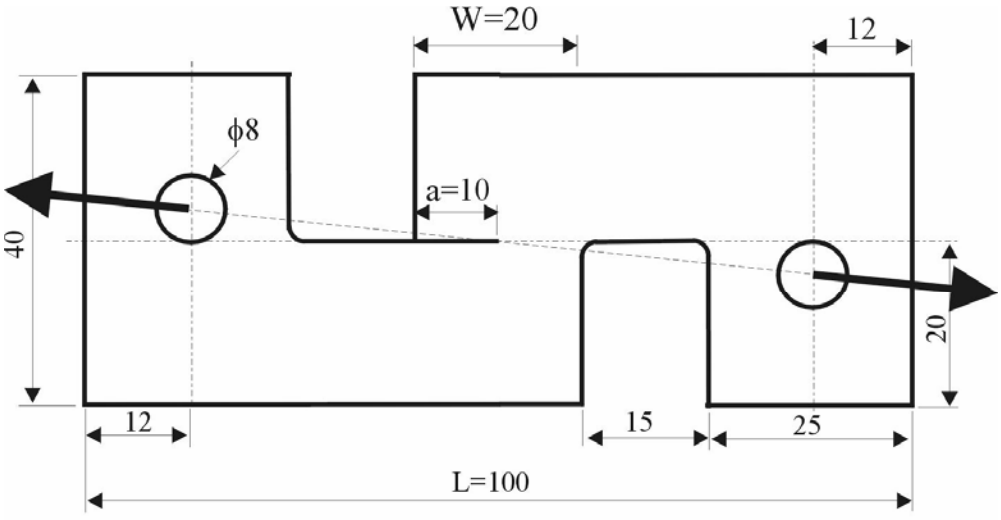

thickness = 20 mm.

FIGURE 2. Mode II specimen.

$$Q_{II} = \frac{\sigma_{\theta\theta} - (\sigma_{\theta\theta})_{REF}}{\sigma_{\circ}} \quad \text{at} \quad \theta = \theta_o \quad \text{for} \quad 1 \le \frac{r\sigma_o}{J} \le 5 \tag{2}$$

Here $(\sigma_{\theta\theta})_{REF}$ is either the HRR solution for $\sigma_{\theta\theta}$ in mode II or the mode II boundary layer solution for small scale yielding (T=0). Using a set of finite element analysis Ayatollahi et al [11] derived the relation between Q and the T-stress for hardening coefficient n=3, 8, 13. Fig. 1 shows the Q-T diagram for n=8 .

Finite Element Modeling

In real specimens, the variation of the constraint parameter Q with load can be determined directly from the near crack tip stresses using finite element results. Alternatively, the Q parameter can be predicted from a Q-T diagram using the value of the T-stress corresponding to the load. In this paper, the variation of Q_{II} with applied load is obtained for a mode II specimen. The specimen, as shown in Fig. 2, is subjected to positive shear for tensile loading and negative shear for compressive loading [12]. The finite element results for Q_{II} are used to study the extent of validity of the results obtained from the Q-T diagram.

The mode II specimen is considered to be elastic-plastic with n=8, α=1.2 in the Ramberg-Osgood stress-strain relation and with Young's modulus E=214 GPa, Poisson's ratio ν=0.3 and yield stress σ_o=400MPa. To calculate the T-stress, the specimen was first simulated by an elastic finite element analysis with the Young's modulus and Poisson's ratio given above. The specimen was subjected to compressive and tensile reference loads of the same magnitude 5 kN. A comparison of the displacement components along the crack faces showed that the mode I stress intensity factor K_I is negligible relative to K_{II}. Therefore, the specimen can be considered as a mode II crack specimen. The J-integral was equal to 2027 N/m for both cases of tensile and compressive loading. The T-stress was determined by using the displacement method described in [10] for mixed mode loading. The value of T-stress for compressive loading was -28 MPa and for tensile loading was +28 MPa. With reference to the sign of the T-stress, in the present analysis the mode II specimen is called a positive T shear specimen for tensile loading and a negative T shear specimen for compressive loading.

Variation of Q_{II} with T for mode II specimen

To study the evolution of crack tip constraint, two finite element analyses are carried out for each loading models: tensile loading and compressive loading. In the first analysis, Q_{II} is determined from a full field solution. The specimen is considered to be elastic-plastic and in the state of plane strain. The shear load is increased beyond the load at which full plasticity takes place in front of the crack tip. The constraint parameter Q_{II} is calculated at r=2J/σ_o along the direction of maximum tangential stress at different load increments throughout the analysis.

For the second analysis the relation between the T-stress and the applied load should be known. Using the reference elastic analysis described in the previous section, the relation between the T-stress and the applied load P_s can be written in general as

$$T = Y_s.P_s \tag{3}$$

where Y_s is a constant factor depending on the type of loading. The factor Y_s is +5.6 and -5.6 MPa/kN for the positive shear and negative shear models, respectively. For the second analysis, the T-stress is determined (using Eq. (3)) at the same loads used to calculate Q_{II} in the first finite element analysis. These values of T are employed to determine Q_{II} from Fig. 1 according to the Q-T diagram for n=8.

Results and Discussion

Fig. 3 shows the results for Q_{II} obtained from the full field solution compared with those determined from the Q-T diagram for the positive T specimen (tensile loading). Similar results are shown in Fig. 4 for the negative T specimen (compressive loading). It is seen in these figures that the results of the two approaches are in good agreement but only for lower load levels. As the load is increased, the difference between the results becomes significant. For loads higher than those to cause full plasticity, the absolute value of Q_{II} drops significantly by increasing load. This is mainly due to the excessive plastic deformation leading to the relief of constraint around the crack tip. It is observed from Figs. 3 and 4 that the extent of agreement between the results of the full field solution and those of the Q-T diagram and also the onset of the drop in the results of the full field solution vary slightly for $+T$ and $-T$ shear specimens.

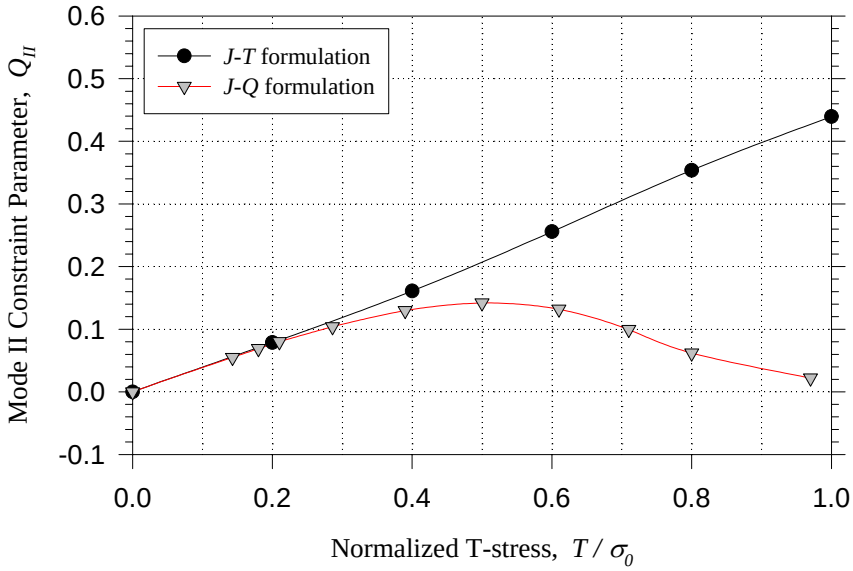

FIGURE 3. Variations of constraint with load for tensile loading.

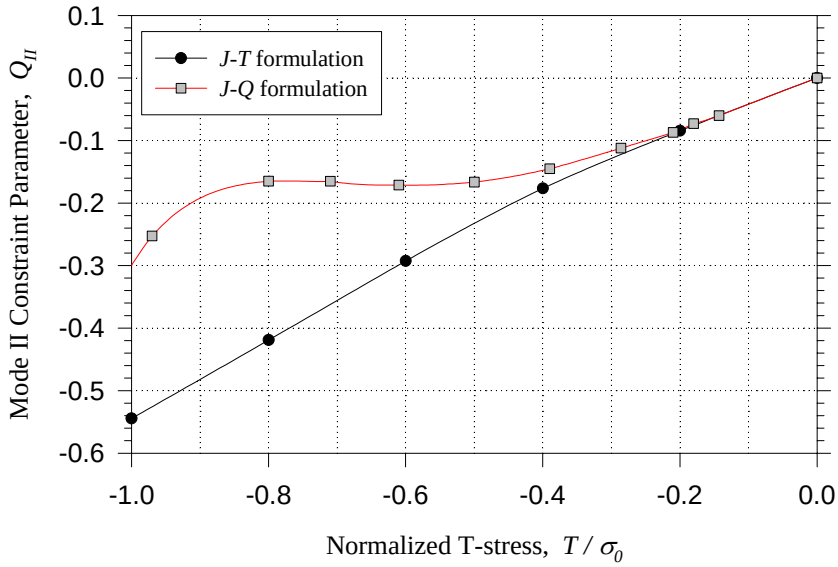

FIGURE 4. Variations of constraint with load for compressive loading.

Figs 5 and 6 display the variation of the tangential stress $\sigma_{\theta\theta}$ normalized with respect to the yield stress σ_o obtained from the first finite element analysis with elastic-plastic behavior for the specimen. Fig. 5 shows the variations of $\sigma_{\theta\theta} / \sigma_o$ with the normalized distance $r\sigma_o/J$ along the direction of maximum tangential stress θ_o for the positive T specimen (tensile loading). Fig. 6 displays similar results but for the negative T specimen. In both figures, the tangential stress has been shown at different levels of load represented here by Log($J/a\sigma_o$) where a is the crack length.

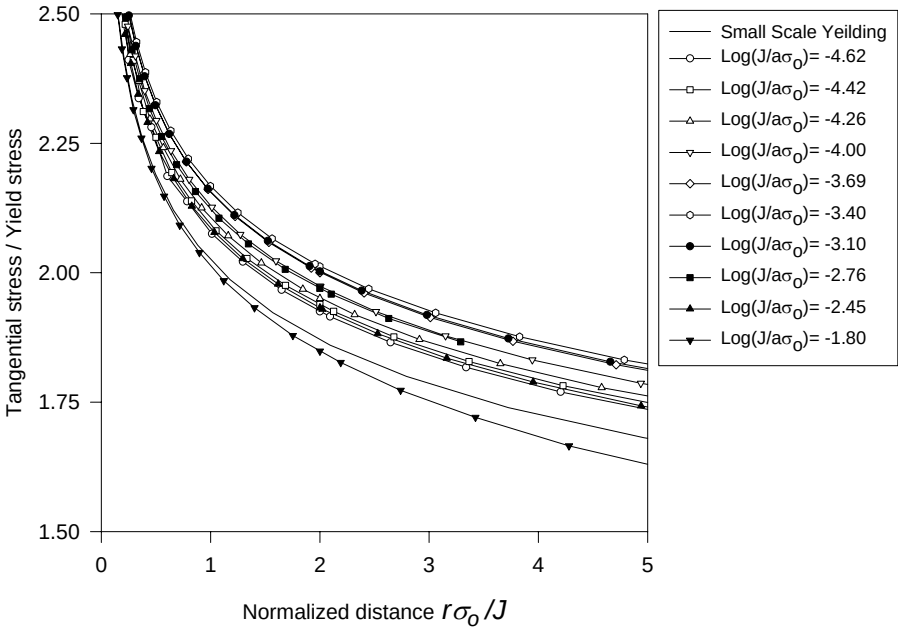

FIGURE 5. Radial variations of tangential stress along θ_o for tensile loading.

For the positive *T* specimen (Fig. 5) the tangential stress initially increases until a load corresponding to Log($J/a\sigma_o$)= -3.4 and then decreases gradually below the small scale yielding solution with *T*=0 (or the HRR solution). The stresses are almost parallel for $1<r\sigma_o/J<5$, although at higher levels of load the stress curves diverge slightly. The change in the stress curves can also be predicted by the results shown in Fig. 3. Since the *T*-stress is positive in tensile loading, the constraint parameter Q_{II} calculated using the *Q*-*T* diagram increases as shown in Fig. 3. However, the *Q*-*T* diagram, obtained for small to moderate scale yielding, does not give accurate results for large scale yielding. Therefore, the *J*-*T* approach cannot be used beyond Log($J/a\sigma_o$) =-3.4 where the tangential stress begins to reduce due to excessive plastic deformation and loss of constraint. The stresses are still parallel up to full plasticity implying that the *J*-*Q* approach is valid for larger extents of plastic deformation. However, for loads higher than that corresponding to full plasticity, the stress curves diverge gradually and the *J*-*Q* approach is not suitable to describe the crack tip stresses.

Fig. 6 shows that for the negative *T* specimen, the tangential stress is always below the HRR solution. The stresses are parallel between $1<r\sigma_o/J<5$ up to Log($J/a\sigma_o$)=-3.1 and diverge considerably beyond it. It is seen from Fig. 4 that again the *J*-*T* approach is valid for small to moderate scale yielding, the *J*-*Q* approach can be used up to full plasticity and that a two-parameter characterisation is no longer applicable beyond the full plasticity.

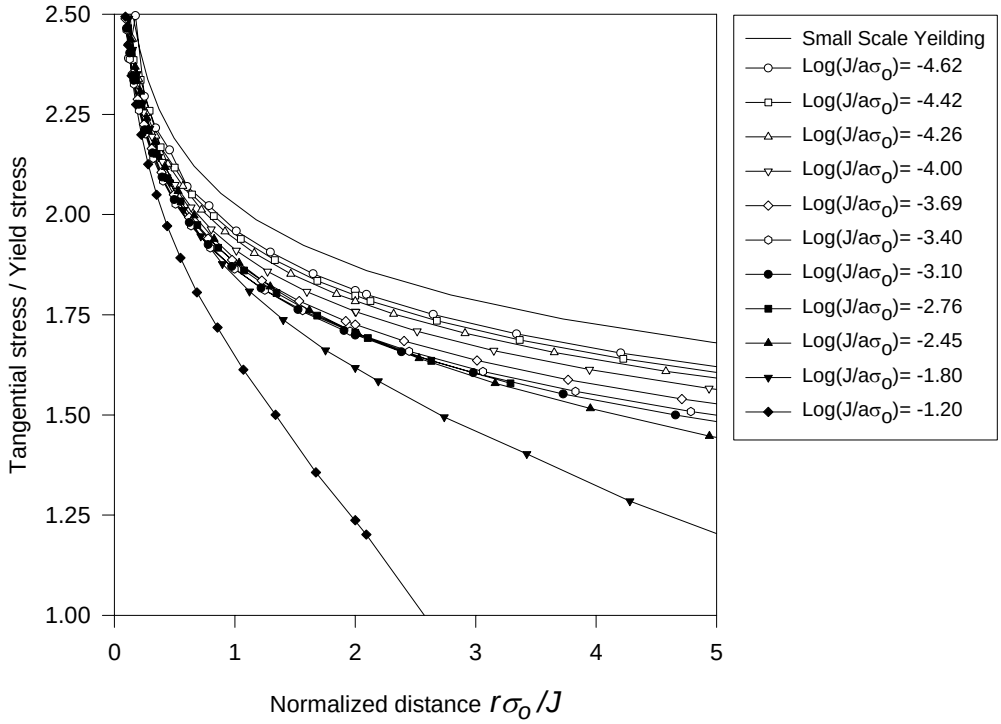

FIGURE 6. Radial variations of tangential stress along θ_o for compressive loading.

Conclusions

- The mode II constraint parameter Q_{II} was determined in terms of T/σ_o for small scale yielding. It can be expected that the mode II fracture toughness in brittle materials increases for shear specimens having a negative *T*-stress and decreases for those having a positive *T*-stress.
- Q_{II} was calculated for two types of shear loading using both the full field solution and the *Q*-*T* diagram. The results of the *Q*-*T* diagram were in agreement with those of the full field solution for small to moderate scale yielding but not for large scale yielding.
- Elastic-plastic finite element analysis of the shear specimen showed that the near crack tip tangential stresses can be predicted for contained yielding using a two-parameter characterization approach. The *J*-*T* approach can be used for small to moderate scale yielding and the *J*-*Q* approach can be used up to full plasticity.

References

1. Maccagno, T.M. and Knott J.F. , *Engng Frac. Mech*. vol. **38**, 111-128, 1991.
2. Erdogan, F. and Sih, G.C., *J. Basic Engng, Tran. of ASME.*, vol. **85**, 519-527, 1963.
3. Maccagno, T.M. and Knott, J.F., *Intl. J. of Frac.*, vol. **29**, R49-R57, 1985.
4. Shih, C.F. and German, M.D. , *Intl. J. of Frac.*, vol. **17**, 27-43, 1981.
5. Betegon, C. and Hancock, J.W., *Journal of Applied Mechanics*, vol. **58**, 104-110, 1991.
6. O'Dowd, N.P. and Shih, F.C., *J. Mech. Phys. Solids*, vol. **39** (8), 989-1015, 1991.
7. O'Dowd, N.P. and Shih, F.C., *J. Mech. Phys. Solids*, vol. **40** (5), 939-963, 1992.
8. Du, Z.Z., Betegon, C. and Hancock, J.W. *Intl. J. of Frac.* vol. **52**, 191-206, 1991.
9. Ayatollahi, M.R., Pavier, M.J. and Smith, D.J., *Intl. J. of Frac.*, vol. **82**, R61-R66, 1996.
10. Ayatollahi, M.R., Pavier M.J. and Smith D.J., *Intl. J. of Frac.*, vol. **91** (3), 283-298, 1998.
11. Ayatollahi, M.R., Smith D.J. and Pavier, M.J., *Intl. J. of Frac.*, vol. **113** (2),153-173, 2002.
12. Ayatollahi, M.R., Pavier, M.J. and Smith D.J., In *Proceedings of 14th European Conference on Fracture*, EMAS Publications, 2002; vol. 1, 161-168.